

High-Energy Femtosecond 1086/543-nm Fiber System for Nano- and Micromachining in Transparent Materials and on Solid Surfaces

S. M. Kobtsev*, S. V. Kukarin, Y. S. Fedotov, and A. V. Ivanenko

Novosibirsk State University, ul. Pirogova 2, Novosibirsk, 630090 Russia

*e-mail: kobtsev@lab.nsu.ru

Received June 24, 2010; in final form, September 18, 2010

Abstract—The first experimental results on a fiber laser system that generates femtosecond pulses with an energy of 1 μJ at a wavelength of 1086 nm and an energy of 300 nJ at a wavelength of 543 nm are presented. The pulse parameters at a wavelength of 1086 nm are optimized with respect to the effective frequency doubling. The high-energy fiber system makes it possible to solve several problems in the femtosecond material processing.

DOI: 10.1134/S1054660X11040049

INTRODUCTION

The focused radiation of femtosecond pulses with a relatively high energy (no less than 100 nJ) makes it possible to create various micro- and nanostructures in glasses, optical crystals, and fibers [1–3] and on metal surfaces [4, 5]. Different physical principles are involved in the formation of such structures in the optical media (e.g., modification of refractive index [6] or ablation [7]) but the corresponding laser sources exhibit similar parameters: the pulse duration ranges from 50 to 500 fs, the focal energy density is no less than 10 mJ/cm² (up to several joules per square centimeter for the recording of structures in optical media), and the repetition rate ranges from 1 kHz to 10 MHz. The development of a femtosecond system with relatively high pulse energy and repetition rate is a topical problem for the femtosecond material processing. Several femtosecond laser systems (especially, solid-state systems [8–11]) provide a relatively high pulse energy at a low repetition rate (less than 100 kHz). Note that a few applications necessitate a repetition rate of greater than 1 MHz [12, 13]. The fiber systems with a pulse energy of greater than 1 μJ and a repetition rate of greater than 1 MHz were demonstrated but the amplification stages of such systems are normally based on exotic fibers with a large effective mode area [14, 15]. An increase in the repetition rate of short pulses to the gigahertz level can be due to the modulation of cw pumping [16] but such an approach is quite rare.

Most works devoted to the above problem are performed at a wavelength of about 800 nm (titanium-sapphire laser) although shorter and longer wavelengths are more appropriate for several media.

In this work, we present the first results on the development of a fiber laser system with wavelengths

of 1086 and 543 nm and pulse energies of 1.0 and 0.3 μJ , respectively, at a repetition rate of 4 MHz.

EXPERIMENT

Figure 1 demonstrates the configuration of the femtosecond laser system that contains a fiber master oscillator, a fiber amplifier, a grating compressor, and a nonlinear crystal for frequency doubling.

A ring Yb-doped-fiber laser in which the mode locking is based on the nonlinear polarization rotation serves as the master oscillator with normal total dispersion and an increased cavity length, which provides a decrease in the pulse repetition rate [17]. For pumping, we employ a diode laser with an output power of up to 10 W at a wavelength of 976 nm with a fiber output that allows the pumping of double-clad active fibers. The laser cavity contains the following fiber elements: active Yb-GTWave fiber with a core diameter of 7 μm and an inner-cladding diameter of 105 μm [18], polarization beam splitter, polarization -maintaining 50% beam splitter, Faraday isolator, two polarization controllers, and an additional fragment of fiber for a decrease in the pulse repetition rate. Thus, the laser has two outputs in which the radiation is linearly polarized.

In the mode-locked laser at a pump power of about 0.5 W, both outputs provide almost identical radiation powers of about 20 mW at a wavelength of about 1086 nm. The pulse repetition rate of the master oscillator is 4 MHz. Figure 2 shows the spectrum and the noncollinear autocorrelation function of the radiation intensity from the output of the 50% beam splitter. On the assumption of the sech^2 pulse shape, the corresponding pulse duration is 4.5 ps.

In the presence of the additional fragment of the 1060XP fiber with a core diameter of 6 μm (single-

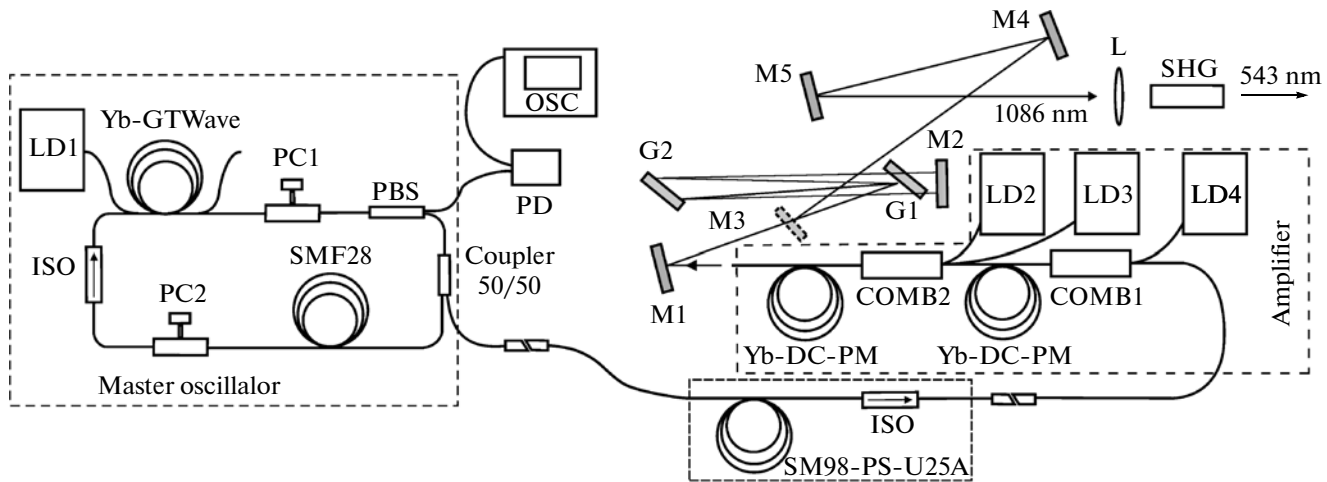


Fig. 1. Block diagram of the high-energy femtosecond fiber system working at wavelengths of 1086 and 543 nm: LD1–LD4, pumping diode lasers, PC1 and PC2, polarization controllers, ISO, Faraday isolator, PBS, polarization beam splitter, PD, control photodetector, M1–M5, totally reflecting mirrors, G1 and G2, diffraction gratings, and SHG, nonlinear crystal for the second-harmonic generation.

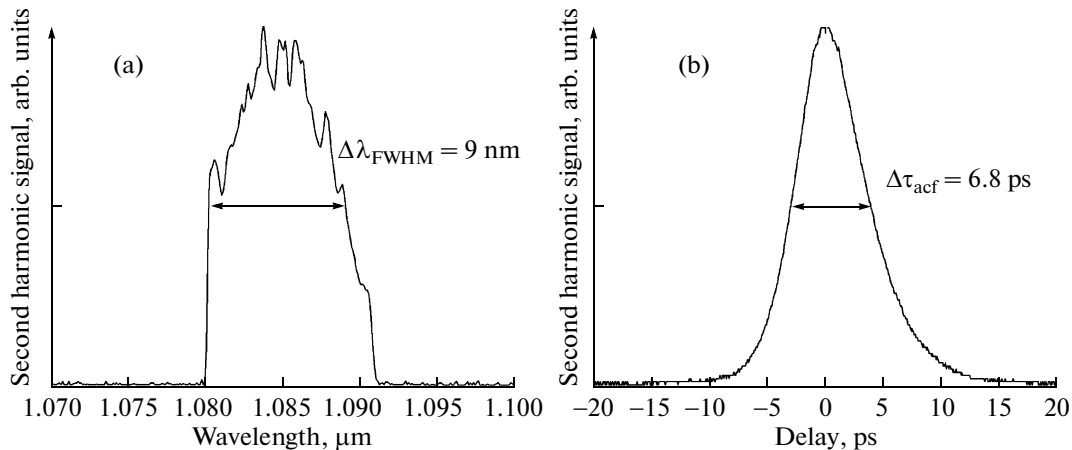


Fig. 2. (a) Spectrum and (b) autocorrelation function of the pulse radiation intensity of the master oscillator.

mode fiber at a wavelength of about $1 \mu\text{m}$), we observe significant (up to 50%) energy conversion of the laser pulses to the Stokes components with wavelengths of about 1140 and 1200 nm. For the generation at a lower repetition rate needed for the further amplification, we substitute the SMF28 fiber with a core diameter of $8.5 \mu\text{m}$ and a length of 40 m for the 1060XP fiber.

The amplification unit contains a fiber isolator, a preamplifier, and an amplifier. In the preamplifier, a polarization maintaining double-clad Yb-doped active fiber with a length of 4 m and a core diameter of $10 \mu\text{m}$ is pumped by a laser diode with a power of up to 9 W using a “ $2 + 1 \times 1$ ” fiber combiner. In the amplifier, a polarization maintaining double-clad Yb-doped active fiber with a length of 2.5 m and a core diameter

increased to $15 \mu\text{m}$ is pumped by two semiconductor diode lasers with a total power of up to 18 W using a similar fiber combiner. The preamplifier provides an increase in the mean power of the master oscillator to a level of about 300 mW. Such an input power of the amplifier is needed for the elimination of the generation of the amplified spontaneous emission, which emerges in the vicinity of the wavelength corresponding to the maximum gain of the active fiber (about 1030 nm) at a relatively high pumping power.

Figure 3 demonstrates the autocorrelation function of the pulse intensity at the output of the amplification unit at a mean power of 1 W. The corresponding pulse duration is 10 ps.

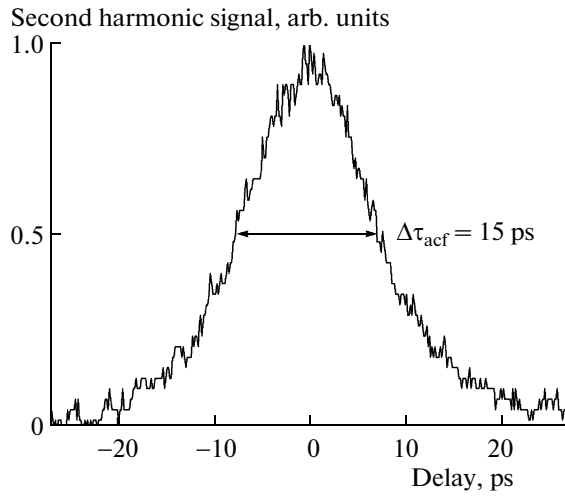


Fig. 3. Autocorrelation function of the pulse radiation intensity for a mean power of 1 W and a wavelength of 1086 nm.

A further increase in the mean power (>1 W) leads to the damage of the output end surface of the fiber in the amplifier. The damage results from the fact that the radiation power density becomes greater than the critical level for the germanosilicate fibers. In accordance with the results from [19], the critical power density is $(2-5) \times 10^9 \text{ W/cm}^2$ for silicate fibers at a cw power of about 1 kW. Using the formula

$$P_c = \frac{P_{av}}{v\Delta\tau S},$$

where P_c is the critical power density of the damage of quartz fiber, $P_{av} = 1 \text{ W}$ is the mean radiation power, $v = 4 \text{ MHz}$ is the pulse repetition rate, $\Delta\tau = 10 \text{ ps}$ is the pulse duration, and $S = 1.8 \times 10^{-10} \text{ cm}^2$ is the area of

the fiber core, we obtain $P_c = 10 \text{ GW/cm}^2$ for a pulse peak power of 2.5 kW.

To decrease the output radiation power density of the amplifier, we decrease the pulse peak power using an increase in the pulse duration (the pulse stretching, amplification, and compression technology). The pulse duration increases due to the presence of the additional SM98-PS-U24A fiber with a length of 5 m. Thus, the mean output power of the amplifier increases to 6–7 W.

For the pulse compression, we use a compressor that consists of two diffraction gratings and additional mirrors with reflectances of about 99.9% for the wavelength range 950–1150 nm. Plane diffraction gratings (1110 mm^{-1}) that work in the Littrow scheme were coated with the reflecting gold layer to provide the stability against radiation damage. The gratings work in the spectral range 1000–1100 nm with an efficiency of 90% for the diffraction in the first order. The total energy efficiency of the compressor is greater than 64%. The maximum output mean power of the compressor is 4.5 W, and the corresponding pulse energy is greater than 1 μJ . Figure 4 shows the spectrum and autocorrelation function of the compressed pulses for a mean power of 4.5 W. The duration of the compressed pulses is 450 fs, and the peak power is 2.2 MW.

For the frequency doubling, we employ the LBO nonlinear crystal with a length of 30 mm that is placed in a high-temperature thermostat and works in the regime of noncritical phase matching. At a mean input power of 1–6 W, the typical efficiency of the frequency doubling is 30–35%. Figure 5 demonstrates the second-harmonic spectrum measured at a mean power of 6 W and a wavelength of 1086 nm.

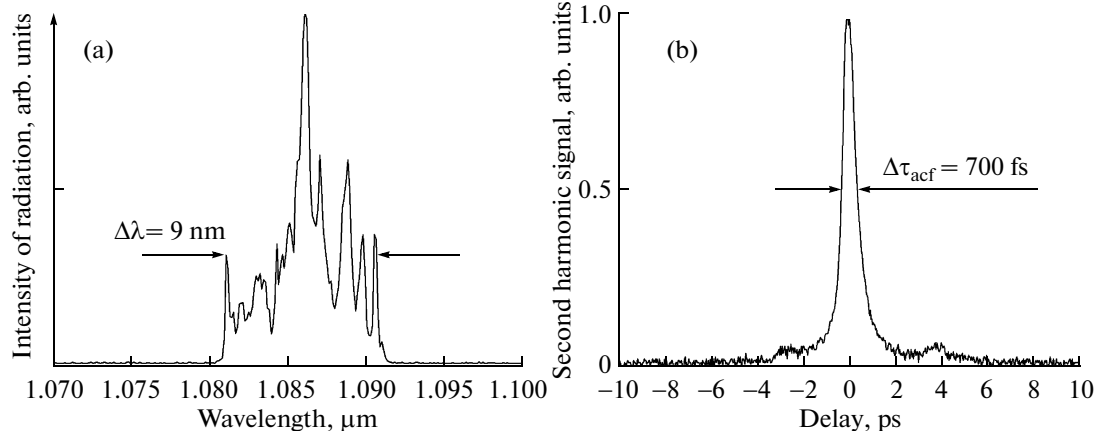


Fig. 4. (a) Spectrum and (b) autocorrelation function of the pulse radiation intensity of the compressor.

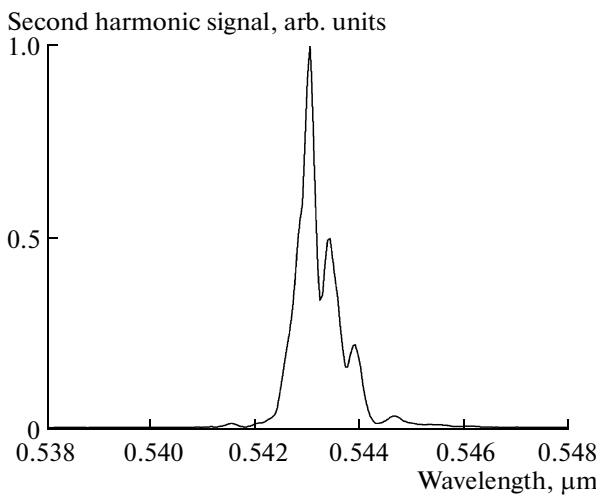


Fig. 5. Spectrum of the second-harmonic radiation of the high-energy femtosecond fiber system for a mean power of 2 W at a wavelength of 543 nm and a pulse energy of 300 nJ.

CONCLUSIONS

We present the high-energy fiber laser system with a relatively high pulse repetition rate (4 MHz), a pulse duration of 450 fs, and pulse energies of greater than 1 μ J and 300 nJ at wavelengths of 1086 and 543 nm, respectively. The system makes it possible to solve several problems of the nano- and micromachining in transparent materials and on solid surfaces. In addition, the radiation parameters at wavelengths of 1086 and 543 nm allow effective parametric conversion to the visible spectral range and to the IR range (up to 2.5–3.0 μ m).

REFERENCES

1. R. R. Gattass and E. Mazur, *Nature Photon.* **2**, 219 (2008).
2. M. Lenzner, J. Krger, S. Sartania, Z. Cheng, C. Spielmann, G. Mourou, W. Kautek, and F. Krausz, *Phys. Rev. Lett.* **80**, 4076 (1998).

3. L. Shah, A. Y. Arai, S. M. Eaton, and P. R. Herman, *Opt. Express* **13**, 1999 (2005).
4. P. Mannion, J. Magee, E. Coyne, and G. M. O'Connor, *Proc. SPIE* **4876**, 470 (2003).
5. N. N. Nedialkov, P. A. Atanasov, S. Amoruso, R. Buzzese, and X. Wang, *Appl. Surf. Sci.* **253**, 7761 (2007).
6. K. M. Davis, K. Miura, N. Sugimoto, and K. Hirao, *Opt. Lett.* **21**, 1729 (1996).
7. E. G. Gamaly, A. V. Rode, B. Luther-Davies, and V. T. Tikhonchuk, *Phys. Plasma* **9**, 949 (2002).
8. F. He, H. S. S. Hung, J. H. V. Price, N. K. Daga, N. Naz, J. Prawiharjo, D. C. Hanna, D. P. Shepherd, D. J. Richardson, J. W. Dawson, C. W. Siders, and C. P. Barty, *Opt. Express* **16**, 5813 (2008).
9. G. Matras, N. Huot, E. Baubéau, and E. Audouard, *Opt. Express* **15**, 7528 (2007).
10. K. H. Hong, T. J. Yu, S. Kostritsa, J. H. Sung, I. W. Choi, Y. C. Noh, D. K. Ko, and J. Lee, *Laser Phys.* **16**, 673 (2006).
11. B.-W. Liu, M.-L. Hu, X.-H. Fang, Y.-Z. Wu, Y.-J. Song, L. Chai, C.-Y. Wang, and A. M. Zheltikov, *Laser Phys. Lett.* **6**, 44 (2009).
12. B. Tan, A. Dalili, and K. Venkatakrishnan, *Appl. Phys. A: Mater. Sci. Process.* **95**, 537 (2008).
13. S. Gaspard, M. Forster, C. Huber, C. Zafiu, G. Trettenhahn, W. Kautek, and M. Castillejo, *Phys. Chem. Chem. Phys.* **10**, 6174 (2008).
14. L. Shah, Z. Liu, I. Hartl, G. Imeshev, G. Cho, and M. Fermann, *Opt. Express* **13**, 4717 (2005).
15. T. Schreiber, C. K. Nielsen, B. Ortac, J. Limpert, and A. Tünnermann, *Opt. Lett.* **31**, 574 (2006).
16. S. M. Kobtsev and S. V. Smirnov, *Opt. Express* **16**, 7428 (2008).
17. S. M. Kobtsev, S. V. Kukarin, S. V. Smirnov, and Y. S. Fedotov, *Laser Phys.* **20**, 351 (2010).
18. A. B. Grudinin, D. N. Payne, P. W. Turner, L. J. A. Nilsson, M. N. Zervas, M. Ibsen, and M. K. Durkin, Patent USA No. 6826335 (Nov. 30, 2004).
19. V. P. Gapontsev and E. Scherbakov, in *Proceedings of the 2nd Intern. Symp. on High-Power Fiber Lasers and Their Applications, St. Petersburg, Russia, 2003* (St. Petersburg, 2003), Paper 2.1.